

# Soil erosion evaluation in a rapidly urbanizing city (Shenzhen, China) and implementation of spatial land-use optimization

Wenting Zhang · Bo Huang

Received: 23 April 2014 / Accepted: 14 August 2014 / Published online: 15 October 2014  
© Springer-Verlag Berlin Heidelberg 2014

**Abstract** Soil erosion has become a pressing environmental concern worldwide. In addition to such natural factors as slope, rainfall, vegetation cover, and soil characteristics, land-use changes—a direct reflection of human activities—also exert a huge influence on soil erosion. In recent years, such dramatic changes, in conjunction with the increasing trend toward urbanization worldwide, have led to severe soil erosion. Against this backdrop, geographic information system-assisted research on the effects of land-use changes on soil erosion has become increasingly common, producing a number of meaningful results. In most of these studies, however, even when the spatial and temporal effects of land-use changes are evaluated, knowledge of how the resulting data can be used to formulate sound land-use plans is generally lacking. At the same time, land-use decisions are driven by social, environmental, and economic factors and thus cannot be made solely with the goal of controlling soil erosion. To address these issues, a genetic algorithm (GA)-based multi-objective optimization (MOO) approach has been proposed to find a balance among various land-use objectives, including soil erosion control, to achieve sound land-use plans. GA-based MOO offers decision-makers and land-use planners a set of Pareto-optimal solutions from which to choose. Shenzhen, a fast-developing Chinese city that has long

suffered from severe soil erosion, is selected as a case study area to validate the efficacy of the GA-based MOO approach for controlling soil erosion. Based on the MOO results, three multiple land-use objectives are proposed for Shenzhen: (1) to minimize soil erosion, (2) to minimize the incompatibility of neighboring land-use types, and (3) to minimize the cost of changes to the status quo. In addition to these land-use objectives, several constraints are also defined: (1) the provision of sufficient built-up land to accommodate a growing population, (2) restrictions on the development of land with a steep slope, and (3) the protection of agricultural land. Three Pareto-optimal solutions are presented and analyzed for comparison. GA-based MOO is found able to solve the multi-objective land-use problem in Shenzhen by making a tradeoff among competing objectives. The outcome is alternative choices for decision-makers and planners.

**Keywords** Soil erosion · Shenzhen · Multi-objective optimization · Land-use change · Geographic information system · Spatial land-use optimization

## Introduction

Soil erosion is a major environmental problem worldwide (Pimentel 1993; Pimentel et al. 1995). It has negative effects on the environment and leads to reduced crop productivity, worsened water quality, lower effective reservoir water levels, flooding, and habitat destruction (Lee 2004; Oh and Jung 2005; Park et al. 2011). Furthermore, soil erosion is considered an essential source of non-point source pollution for the water bodies in many terrestrial environments (Ning et al. 2006; Wu et al. 2012). Additionally, because erosion leads to the removal of the soil's organic carbon and clay content, eroded sediments transporting as much as 20 % carbon can be released into the atmosphere as CO<sub>2</sub> (Lal 1995; Lal and Bruce

---

Responsible editor: Michael Matthies

W. Zhang

Collage of Resources and Environment, Huazhong Agricultural University, Wuhan, China

W. Zhang · B. Huang (✉)

Department of Geography and Resource Management, The Chinese University of Hong Kong, Hong Kong, China  
e-mail: bohuang@cuhk.edu.hk

B. Huang

Institute of Space and Earth Information Science, The Chinese University of Hong Kong, Hong Kong, China

1999; Yang et al. 2003), thereby reducing soil's ability to mitigate the green house effect (Yang et al. 2003).

Soil erosion's negative effects on the environment render it necessary to evaluate and control it. Soil erosion was traditionally considered a purely natural process caused by rainfall and water flow. However, human activities have recently greatly aggravated such erosion through alteration of the land cover and disturbance of the soil structure (Yang et al. 2003). It is estimated that nearly 60 % of present soil erosion is induced by human activities (Yang et al. 2003). Accordingly, numerous studies have attempted to estimate soil erosion with regard to the effects of these activities, many of them taking the form of analyses of how land-use changes, as a direct and visible reflection of human activities, affect soil erosion (Meyer and Turner 1994). Land-use changes such as urban sprawl and the disappearance of forest, water bodies, and grasslands reflect the extent and intensity of human activities. Thanks to such technological developments as the geographic information system (GIS) and remote sensing (RS), it is now easy to collect land-use change data, which is beneficial to soil erosion studies. Numerous soil erosion evaluations based on land-use changes have now been carried out with GIS and RS assistance. For example, Zhou et al. (2008) collected land-use data in the southwestern Chinese city of Chongqing from RS images and analyzed the city's annual soil erosion on the basis of these changes. Their results indicated a high risk of soil erosion in agricultural areas with frequent human activities. Van Hengstum et al. (2007) estimated the effects of land-use patterns and urbanization on wetland and sedimentation patterns in Frenchman's Bay in the U.S. state of Maine and found an increased input of fine-grained sediments into wetlands to result in reduced water clarity. Fistikoglu and Harmancioglu (2002) reported that the quantity and quality of soil properties, land use, and vegetation reflect difficulties in the application of soil erosion methodology. Yang et al. (2003) employed a GIS-based revised universal soil loss equation model to evaluate global soil erosion with regard to global land-use patterns and climate change. They estimated that, with the development of cropland in the past century, the soil erosion potential worldwide has increased by about 17 %. Similarly, Lufafa et al. (2003) examined soil loss on different land-use types and found the greatest such loss to be predicted for cropland, followed by rangeland.

Although numerous soil erosion studies taking the effects of land-use changes into account have been carried out, with meaningful outcomes achieved, most stop at evaluation. Studies on how to achieve appropriate land-use allocation planning to control soil erosion are limited in number. What makes further studies in this arena particularly difficult is that land-use allocation decisions are driven by social, economic, and environmental factors at the same time. They cannot be determined by considering soil erosion control in isolation.

Optimization methods have long been used to address these problems and formulate comprehensive land-use plans. As long ago as the 1960s, the linear programming (LP) optimization model was articulated to solve linear or quadratic equations to address problems in urban planning systems (Guldman 1979; Aerts et al. 2003). However, the LP model cannot handle nonlinear and unstructured requirements such as the spatial interactions among land-use types, and it is thus unsuitable for complex urban problems. In addition, land-use planning systems involve multiple objectives, and LP is efficient only when a single objective has been identified (Stewart et al. 2004). To address these issues, a genetic algorithm (GA)- and heuristic algorithm-based multi-objective optimization (MOO) approach capable of handling unstructured urban issues was proposed in the 1970s (Hopkins 1977; Los 1978). The GA is a type of general global optimization algorithm that has been shown to be robust and efficient for searching large, complex, and little-understood search spaces such as those of multi-objective land-use planning problems (Zhang et al. 2010). Furthermore, because the GA works with a population of plans, a number of Pareto-optimal solutions can be generated. These solutions are defined as the subset comprising the non-dominant designs in the generation (Balling and Wilson 2001), where a solution is dominant if another solution exists that is better than or equal to it in every objective and better than it in at least one objective. By obtaining a set of Pareto-optimal solutions, land-use planners and decision-makers can choose from a set of alternative plans rather than one "best" plan. The Pareto-optimal solutions generated by the GA are well suited for practical applications. Owing to its advantages in addressing the multi-objective problems inherent in land-use planning, the GA is widely used by scholars to formulate optimal land-use plans. A number of meaningful outcomes have been achieved, and GA-based MOO is considered a useful tool in land-use planning. For example, Balling et al. (1999a, b) used the GA to search for optimal future land-use and transportation plans for a high-growth city, which allowed the decision-makers involved to value each plan in the Pareto-optimal set by assigning a relative importance to each objective. Stewart et al. (2004) developed a special purpose GA for the solution of nonlinear combinatorial optimization problems in land-use planning systems. Their proposed GA was applied to a specific land-use planning problem in The Netherlands, and their results indicated its efficacy for land-use planning and decision support systems. Cao et al. (2012) developed a boundary-based fast genetic algorithm to search for optimal solutions to a land-use allocation problem. Finally, Holzkämper and Seppelt (2007) confirmed the GA's efficacy in supporting management decisions. They also pointed out that the GA-based MOO approach can be used as an extension to the GIS and for spatially explicit decision support tools.

MOO has achieved great success in generating optimal land-use plans. However, few scholars have considered soil erosion control as an objective in MOO, as such control constitutes a complex spatial problem with many factors. The study reported herein adopted a well-developed soil erosion evaluation model, the universal soil loss equation (USLE) model proposed by Wischmeier and Smith (1961), to assess the objective of soil erosion control. The GIS and RS techniques were also used to assist in the soil erosion evaluation. To validate the efficacy of the MOO approach, Shenzhen, a rapidly urbanizing city in south China, was selected as the case study area. The MOO approach was used to search for sound land-use plans for the city in 2020. Referring to a textbook on Shenzhen’s overall land-use plan and the city’s development trend, four land-use constraints and three land-use objectives were defined. The objectives were (1) minimizing soil erosion, (2) minimizing the incompatibility of neighboring land-use types, and (3) minimizing the cost of a change to the status quo.

**Study area and data**

Shenzhen (22°27’N to 22°52’N, 113°46’E to 114°37’E) is located in the eastern part of the Pearl River Delta region adjacent to Hong Kong (Fig. 1) and has a total terrestrial area of 1,952.84 km<sup>2</sup>. Owing to its proximity to Hong Kong, the then-small fishing village was designated the Shenzhen Special Economic Zone (SSEZ) in 1980 and, in the years since, has experienced rapid urbanization and economic growth (Chen et al. 2012). It is now a major economic center (Chen et al. 2012). Shenzhen features numerous mountainous areas with a steep slope (Chen et al. 2012). In fact, land with an elevation greater than 80 m accounts for about 30 % of the total area of the SSEZ, although the lowest elevation

is 0 m. Shenzhen has a subtropical monsoon climate with abundant rainfall. Because soil erosion can be defined as a process by which soil is washed away by the flow of water, steeper slopes and abundant rainfall are aggravating factors (Lee 2004; Dumas et al. 2010). Given these natural land characteristics, Shenzhen is vulnerable to severe soil erosion. Chen et al. (2001) reported that 97.3 km<sup>2</sup> of land in Shenzhen suffered soil erosion in 1998, accounting for 4.98 % of the SSEZ’s total land area.

In addition to its natural characteristics, the rapid land-use changes that Shenzhen has undergone in the past 20 years have further exacerbated its soil erosion. In that period, the city’s urban area has expanded enormously, with a concomitant decrease in cropland, forest area, and water bodies (Li et al. 2010). The land-use data used in this study (see Table 1 and Fig. 2) were obtained from the Shenzhen Bureau of Land and Resources. They cover eight land-use types: cultivated land, garden plots, grassland, built-up land, land for transportation, water bodies, forest, and unused land. Table 1 shows the quantitative land-use changes in Shenzhen from 1996 to 2008. It can be seen that built-up land and land for transportation have experienced the sharpest increases, accompanied by a decrease in the other land-use types. The land-use change data clearly illustrate the rapid process of urbanization that Shenzhen underwent in the 12-year period considered.

**Methods**

Soil erosion evaluation

The now well-known USLE model was first proposed by Wischmeier and Smith (1961) and has since become one of

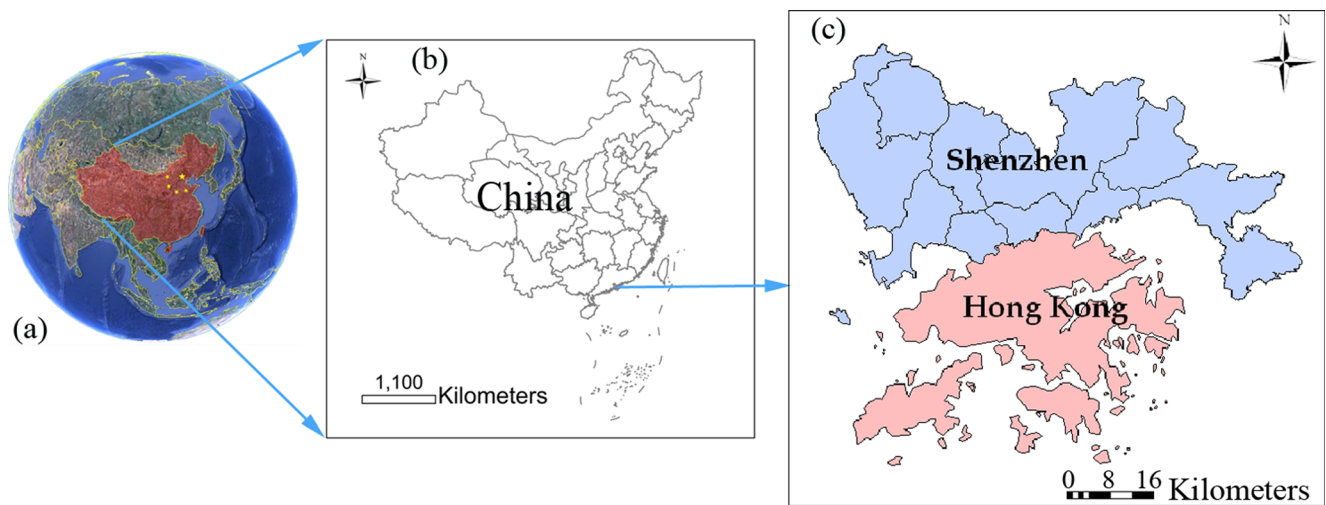


**Fig. 1** Research area: **a** the location of China on the globe, **b** location of Shenzhen in China, and **c** administrative district maps of Shenzhen and Hong Kong

**Table 1** Land-use changes in Shenzhen from 1996 to 2008

Land-use type	1996	2000	2002	2004	2006	2008
	Area (km <sup>2</sup> )					
Cultivated land	67.42	74.48	59.78	46.93	42.49	32.06
Garden plot	214.62	272.30	301.61	277.80	264.08	231.46
Forest	727.41	649.99	648.27	636.25	629.36	594.41
Grassland	3.90	0.39	0.73	0.47	1.39	2.61
Built-up land	434.85	489.03	571.71	642.95	676.92	754.43
Transportation	118.61	134.43	123.17	136.25	143.62	187.38
Water body	229.52	221.95	223.28	195.45	182.70	141.34
Unused land	156.50	110.28	24.29	16.73	12.26	9.14
Sum	1,952.84					

the most widely used and empirically grounded approaches (Ozcan et al. 2008; Meusburger et al. 2010; Abu Hammad 2011). It consists of a set of calculations to estimate the soil erosion on a plot of land with homogeneous characteristics (Wischmeier and Smith 1978). In the USLE model, the average annual soil loss is based on the product of five erosion risk indicators (Meusburger et al. 2010):

$$A = R \times K \times LS \times C \times P, \quad (1)$$

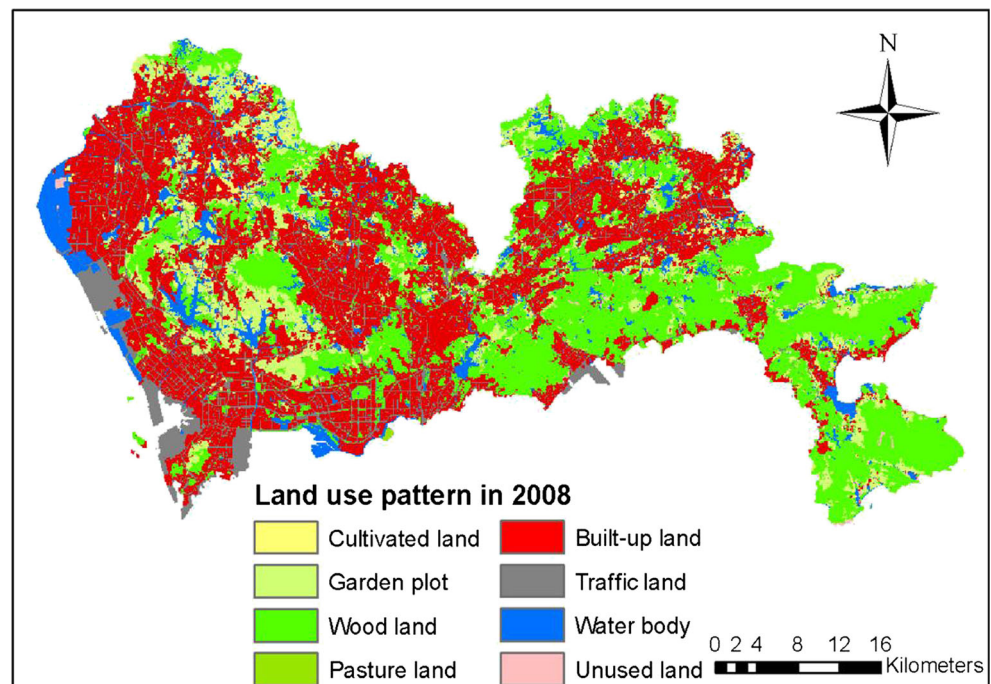
where  $A$  (tonnes per hectare per year) is the predicted average annual soil loss,  $R$  (megajoule millimeters per hectare per hour per year) is the rainfall and runoff factor,  $K$  (tonnes per hectare per unit  $R$ ) is the soil erosivity factor,  $LS$  (dimensionless) is the slope length and steepness factor,  $C$  (dimensionless) is the cover and

management factor, and  $P$  (dimensionless) is the conservation practices factor. The  $R$ ,  $K$ , and  $LS$  factors basically determine the erosion volume, whereas the  $C$  and  $P$  factors are reduction factors ranging from 0 to 1 (Kumar and Kushwaha 2013). Among all these factors,  $R$ ,  $K$ , and  $LS$  factors are not varying with land-use change. On the other hand, the  $P$  factor reflects the impact of land-use changes, with one land-use type maintaining a unique  $P$  factor; meanwhile  $C$  factor is determined according to the vegetable coverage, which also has been impacted by land-use change. Since the  $P$  factor and  $C$  factor are varying with land-use change, the USLE model thus allows the influence of land-use change on soil erosion to be reflected. In this study, the impact of land-use changes on soil erosion is focused.

**Rainfall and runoff factor:  $R$**  The rainfall and runoff factor ( $R$ ) represents two characteristics of a storm that determine its erosivity: the amount of rainfall and peak intensity sustained over an extended period. Drawing on Li et al. (2009),  $R$  can be calculated by the following equation.

$$R = \sum_{k=1}^{12} (0.3046P_k - 2.6398) \quad (2)$$

In Eq. 2,  $R$  is the rainfall and runoff factor (megajoule millimeters per hectare per hour per year), and  $P_k$  is the average monthly rainfall (millimeters) (Kim et al. 2005). Table 2 lists the annual rainfall (Shenzhen Statistics Bureau,

**Fig. 2** Spatial distribution of the land-use pattern in 2008

**Table 2** Annual precipitation and *R* factors for Shenzhen from 1996 to 2008

Year	Annual precipitation (mm)	<i>R</i> factor (MJ mm ha <sup>-1</sup> h <sup>-1</sup> year <sup>-1</sup> )
1996	1,683.3	481.06
2000	2,533.6	740.06
2002	1,882.8	541.82
2004	1,299.4	364.12
2006	1,936.5	558.18
2008	2,710	793.79

1997, 2001, 2003, 2005, 2007, 2009) in 1996, 2000, 2002, 2004, 2006, and 2008 and the corresponding values of the *R* factors for Shenzhen in various years.

The value of the *R* factor for Shenzhen can be obtained from Eq. 2. However, this *R* factor is constant for the whole of Shenzhen and does not reflect spatial differences. Therefore, the spatial distribution of the annual average rainfall for numerous years is used to spatialize it (see Eq. 3). More specifically, this spatial distribution is achieved by interpolation, as the annual average rainfall for numerous years is available at each monitoring station.

$$R_{(mx,ny)} = \frac{\text{AnAvRainfall}_{(mx,ny)} - \min(\text{AnAvRainfall})}{\max(\text{AnAvRainfall}) - \min(\text{AnAvRainfall})} R \quad (3)$$

In Eq. 3,  $R_{(mx,ny)}$  is the value of the refined *R* factor at the location of grid  $(mx,ny)$ ,  $\text{AnAvRainfall}_{(mx,ny)}$  is the value of the annual average rainfall for numerous years at grid  $(mx,ny)$ ,  $\min(\text{AnAvRainfall})$  and  $\max(\text{AnAvRainfall})$  are the minimum and maximum of the annual average rainfall for numerous years in the entire city, and *R* is the rainfall and runoff factor calculated by Eq. 2. Finally, with the assistance of the GIS tool, the *R* factor with spatial information is achieved. Figure 3a shows the spatial distribution of the *R* factor in 2008 as an example.

**Soil erosivity factor: *K*** The soil erosivity factor is defined as the rate of soil loss per unit of *R* as measured on a unit plot (Wischmeier and Smith 1978; Ozsoy et al. 2012) and represents the average long-term soil and soil profile response to the erosive power associated with rainfall and runoff (Lee 2004). The *K* factor is determined by the soil’s physical and chemical properties, which vary from place to place. Several experimental models have been established on the basis of soil texture, organic matter, structure, and osmosis (Wischmeier 1976; Wischmeier and Smith 1978). In the current study, the

value of *K* is determined by the following equation given by Sharpley and Williams (1990).

$$K = \{0.2 + 0.3\exp[-0.0256w_d(1-w_i/100)]\} \times \left(\frac{w_i}{w_l + w_i}\right)^{0.3} \times \left\{1.0 - \frac{0.025w_c}{w_c + \exp(3.72-2.95w_c)}\right\} \times \left\{1.0 - \frac{0.7w_n}{w_n + \exp(-5.51 + 2.29w_n)}\right\} \quad (4)$$

where  $w_d$  is percent sand,  $w_i$  is percent silt,  $w_l$  is percent clay,  $w_c$  is percent organic matter, and  $w_n$  is the factor that is determined by percent sand using the formulation  $w_n = (1 - \frac{w_d}{100})$  (Sharpley and Williams 1990; Zhou et al. 2008). All of the soil characteristic data used in Eq. 4 are available from the Food and Agriculture Organization of the United Nations (Nachtergaele et al. 2008). The spatial distribution of the *K* factor for Shenzhen is obtained using Eq. 4 and the GIS tool and is presented in Fig. 3b. Some areas of Shenzhen lack soil type data. The *K* factors for these areas are represented as ‘no data’ and were omitted during the soil erosion evaluation.

**Slope length and steepness factor: *LS*** The slope length and steepness factor (*LS*) represents the effect of the topography on soil erosion (Lufafa et al. 2003), as an increase in slope length and steepness produces higher overland flow velocities and therefore stronger erosion (Dumas et al. 2010). *LS* is derived from Eq. 5, as follows.

$$LS = \left(\frac{\lambda}{22.13}\right)^m \times (65.41\sin^2\theta + 4.56\sin\theta + 0.0065) \quad (5)$$

where  $\lambda$  is the slope length in meters,  $\theta$  is the slope angle in degrees, and  $m$  is a slope angle contingent variable (McCool et al. 1987) that can be calculated by

$$m = \begin{cases} 0.3 & 22.5^0 \leq \theta \\ 0.25 & 17.5^0 \leq \theta < 22.5^0 \\ 0.2 & 12.5^0 \leq \theta < 17.5^0 \\ 0.15 & 7.5^0 \leq \theta < 12.5^0 \\ 0.10 & \theta < 7.5^0 \end{cases} \quad (6)$$

The coefficients of  $\lambda$  and  $\theta$  are obtained from the digital elevation model, the resolution of which is 30 by 30 m. Finally, based on these equations, the spatial distribution of the *LS* factor for Shenzhen is obtained and is represented in Fig. 3c.

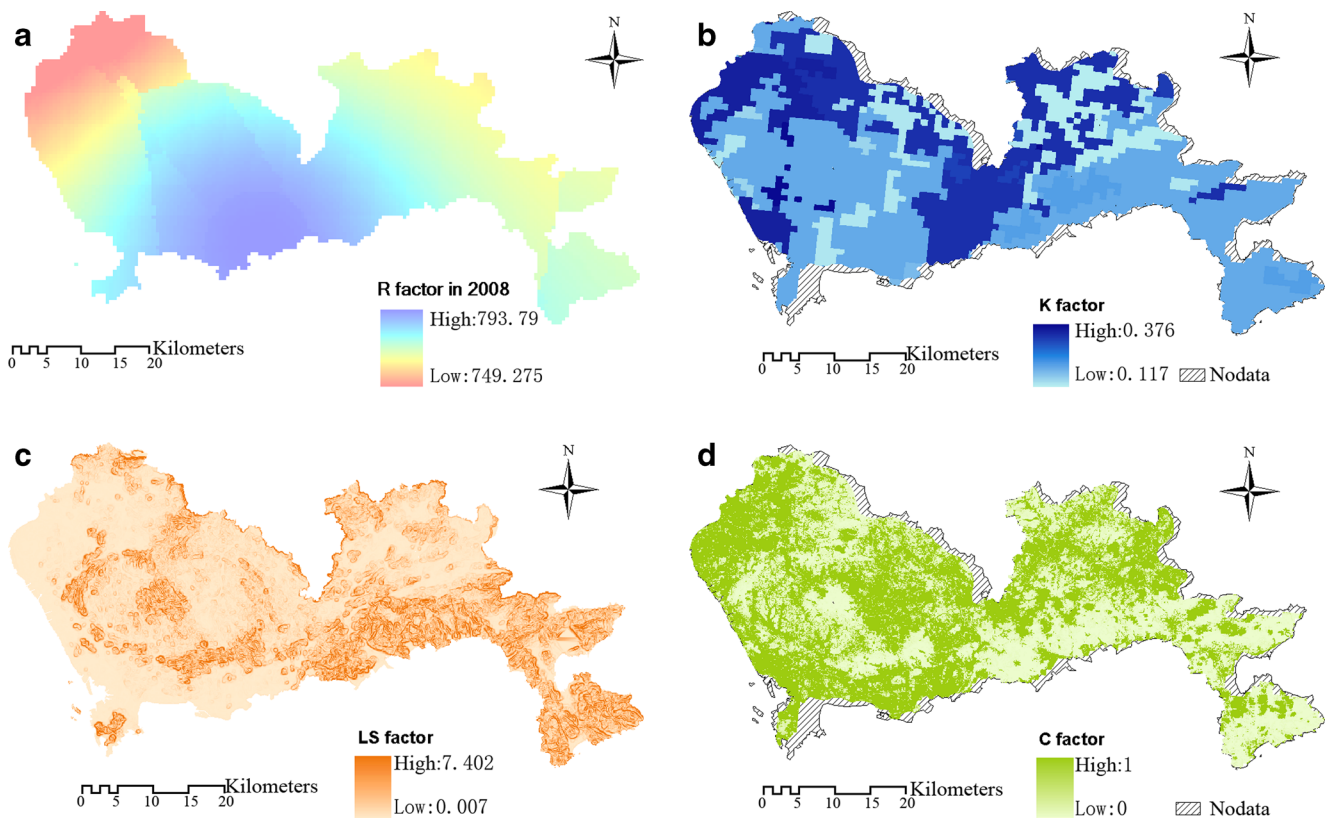


**Fig. 3** Spatial distribution of USLE factors in Shenzhen. **a** *R* factor in 2008. **b** *K* factor. **c** *LS* factor. **d** *C* factor

**Crop and management factor: *C*** The crop and management factor *C* depends on vegetation cover, which dissipates the kinetic energy of raindrops before they hit the soil surface. Erosion and runoff are markedly affected by different types of vegetation cover. Erosion and runoff is measured as the ratio of soil loss to land cropped under continuously fallow conditions (Wischmeier and Smith 1978). According to this definition, *C* equals 1 when it is subject to standard fallow conditions. As the percentage of vegetation cover approaches 100 %, the *C* factor value approaches the minimum. The *C* factor can be calculated by Eq. 7, as follows (Cai et al. 2000; Ma et al. 2001; Zhao et al. 2007) and *lc* by the normalized differential vegetation index (*NDVI*) (see Eq. 8) (Ma et al. 2001).

$$C = \begin{cases} 1 & lc = 0 \\ 0.6805 - 0.3436 \lg lc & 0 < lc < 78.3\% \\ 0 & 78.3\% \leq lc \end{cases} \quad (7)$$

$$lc = (108.49NDVI + 0.717)/100 \quad (8)$$

where *lc* (dimensionless) is vegetation coverage, and *NDVI* (dimensionless), which ranges from  $-1$  to  $1$ , can be obtained from the RS image. An *NDVI* value approaching 1 indicates that the land is fully covered by vegetation, leading to a high value for *lc*. Using the foregoing equations, the spatial distribution of the *C* factor for Shenzhen is obtained, as shown in Fig. 3d. Some plots in Shenzhen have no data for the *C* factor, and their *C* factors were thus omitted from the soil erosion evaluation.

**Conservation practice factor: *P*** Conservation practice factor *P* is defined as the ratio of soil loss from the upward and downward slope of an inclined plane where a soil preservation policy has been put in place (Park et al. 2011). In fact, the *P* factor affects erosion by redirecting runoff around the slope to produce less erosivity or slowing down the runoff to make a deposition (Lee 2004). Its value ranges from 0 to 1, with a lower value suggesting more effective conservation practices. According to the literature (Xu and Li 1999; Yang et al. 2003; Zhao et al. 2007; Mu et al. 2010; Park et al. 2011; Kumar and Kushwaha 2013), the *P* factor is associated with the land-use type and is a reflection of land-use changes. The value of the *P* factor for each type of land-use in Shenzhen is determined (Table 3) with reference to the literature (Mu et al. 2010; Ozsoy et al. 2012).

Spatial land-use optimization

Constraints

Shenzhen is undergoing a dramatic process of urbanization accompanied by an increase in built-up areas. From the perspective of the city’s current development trend, a sustainable urbanization process is required to satisfy the needs of the growing economy and mitigate environmental problems. According to local policy and the economic growth model, the four following constraints are proposed.

- (1) Built-up area should be around 990 km<sup>2</sup>  
 According to Shenzhen’s land-use plan for 2006 to 2020, and from the aspect of land resource protection, however, the built-up area should total 990 km<sup>2</sup> by 2020. Thus, with reference to the suggestions of urban planners and decision-makers, we decided that the area of built-up land should be around 990 km<sup>2</sup>, in projected year 2020, which should provide sufficient land for economic development and population growth.
- (2) Water body=141.34 km<sup>2</sup>  
 The local environmental policy states that the water body should not be occupied by built-up land during the urbanization process. Therefore, in 2020, the water body should be maintained at 141.34 km<sup>2</sup>, its total area in 2008.
- (3) Cultivated land ≥ 25.65 km<sup>2</sup>  
 According to China’s national Basic Farmland Protection Regulations, basic farmland in Shenzhen should not be less than 80 % of total cultivated land. Basic farmland is a type of cultivated land that should be maintained and protected according to national policy. Hence, the amount of cultivated land in 2020 should be equal to or greater than 32.06 × 0.8=25.65 km<sup>2</sup>.
- (4) Elevation<80 m  
 Shenzhen is a mountainous area with ecological forest cover and is thus difficult to develop. The city’s land-use

plan for 2006–2020 states that land with an elevation greater than 80 m is protected from development.

Objectives

After defining the foregoing constraints, the following land-use objectives are proposed.

- (1) Minimize soil erosion:  

$$\min Z_{\text{soil erosion}} = R \times K \times LS \times C \times P \tag{9}$$
- (2) Minimize the incompatibility of neighboring land-use types

In the real world, a given land use such as industrial land tends to be clustered, a phenomenon we call zoning or clustering but which can also be defined as the compatibility of land use. Land-use compatibility can minimize conflicts with neighboring land uses (Ligmann-Zielinska et al. 2008) and can also result in the effective utilization of available land (Cao et al. 2012). Furthermore, ensuring the compatibility of neighboring land-use types is critical to enhancing accessibility and reducing resource consumption. Therefore, maximizing land-use compatibility, or minimizing incompatibility, is an important objective in land-use planning.

Each land-use type has a preferred location, and various such preferences can be used to measure the degree of incompatibility. For example, the preferred location for a given built-up land plot is close to another built-up land plot. If the plot is instead surrounded by cultivated land, then its location is not conducive to future development. In this paper, the degree of conflict between two land-use types is used to measure the degree of incompatibility. The degree of conflict ranges from 0 to 1, with a higher value indicating greater conflict between two land-use types. In determining the degree of conflict, in addition to reference to previous studies (Ligmann-Zielinska et al. 2005; Cao et al. 2011, 2012), we adopt the analytic hierarchy process (Tsyganok et al. 2012) to collect and analyze the suggestions of experts, decision-makers, and various stakeholders. The final degrees of conflict are presented in Table 4, and the objective of minimizing the incompatibility of neighboring land-use types is represented by Eq. 10.

$$\min Z_{InCom} = \sum_{l \in U} \sum_{j \in I} \text{ConflictDegree}(\text{plot}_l, \text{plot}_j) \tag{10}$$

where  $Z_{Incom}$  is the incompatibility of the  $i$ -th plan,  $\text{plot}_l$  and  $\text{plot}_j$  are the  $l$ -th and  $j$ -th plots in the  $i$ -th plan,

**Table 3**  $P$  factors for different land-use types in Shenzhen

Land-use type	$P$ factor
Cultivated land	0.5
Garden plot	0.6
Forest	1.0
Grassland	1.0
Built-up land	0.3
Transportation	0.3
Water body	0
Unused land	1

**Table 4** Degrees of conflict between land-use pairs

	Cultivated land	Garden plot	Forest	Grassland	Built-up land	Transportation	Water body	Unused land
Cultivated land	0	0.1	0.2	0.3	0.8	0.7	0.2	0.1
Garden plot	0.1	0	0.1	0.1	0.7	0.6	0.1	0.1
Forest	0.2	0.1	0	0.2	0.7	0.6	0	0.1
Grassland	0.3	0.1	0.2	0	0.6	0.6	0	0.1
Built-up land	0.8	0.7	0.7	0.6	0	0	0.6	0.5
Transportation	0.7	0.6	0.6	0.6	0	0	0.5	0.1
Water body	0.2	0.1	0	0	0.6	0.5	0	0.1
Unused land	0.1	0.1	0.1	0.1	0.5	0.1	0.1	0

respectively, and  $I_l$  is the neighborhood in which plot  $l$  is located.

(3) Minimize the cost of changes to the status quo

The cost of changes to the status quo is measured by the cost of developing a plot from one land-use type to another (Zhang et al. 2010). In this paper, a dimensionless changing cost factor is used to denote the per unit area cost of such development. Because that factor reflects only the relative relationship between different kinds of land-use change or conservation, it is simple and helps to avoid error in determining the real cost. Then, the cost of a change to the status quo for a given land-use plan can be obtained by summing the product of the changing cost factor and changed area. To determine the changing cost factor of each land-use pair, we drew upon the literature (Ligmann-Zielinska et al. 2005; Cao et al. 2011, 2012) and took into account the suggestions of experts, decision-makers, and stakeholders in the land-use allocation. The cost of changing from one land-use type to another was determined by a specialist and professionals. The outcomes are listed in Table 5, and the objective of minimizing the cost of changes to a given plan is represented by Eq. 11.

$$\min Z_{\text{change}} = \sum_{\text{Plot}_j \in U} \text{ChangeCost}_{lm2ln} * \text{Area}(\text{Plot}_j) \quad (11)$$

where  $Z_{\text{change}}$  is the cost of a change to the status quo, i.e., plan  $i$ ;  $\text{Plot}_j$  denotes a plot whose land use has changed from the status quo, the  $lm$ -th land-use type, to another type, the  $ln$ -th land-use type, in plan  $i$ ; and  $\text{ChangeCost}$  is the changing cost factor listed in Table 5.

### Optimization

A GA-based MOO technique was used to search for optimal land-use allocations for Shenzhen. Land-use zones (LUZs), which are divided by the road network and contour lines, act as the genes in the GA process. In some studies, the road network alone, described as the traffic analysis zone, is used to divide LUZs (Balling et al. 2004). However, Shenzhen, the site of our case study, has many mountainous areas that the road network does not reach. Accordingly, we use the road network associated with contours of 75-m intervals to separate the LUZs (see Fig. 4). There are 10,742 LUZs in Shenzhen, each of which maintains one and only one land-use type. Of these, 778 are covered by a water body and 2,223 feature an average elevation greater than 80 m, on which development is restricted. These LUZs cannot be changed in the future. Therefore, only  $10,742 - 778 - 2,223 = 7,741$  LUZs or genes are optimized by the GA. The optimization space and cost of optimization are thus reduced.

**Table 5** Cost of changing from one land-use type to another

Change to/ change from	Cultivated land	Garden plot	Forest	Grassland	Built-up land	Transportation	Water body	Unused land
Cultivated land	0	0.3	0.3	0.3	0.6	0.7	0.1	0.1
Garden plot	0.4	0	0.2	0.2	0.6	0.6	0.1	0.1
Forest	0.4	0.2	0	0.2	0.7	0.6	0.1	0.1
Grassland	0.4	0.2	0.2	0	0.6	0.6	0.1	0.1
Built-up land	1	1	1	1	0	0.5	1	0.9
Transportation	1	1	1	1	0.5	0	1	1
Water body	1	1	1	1	1	1	0	1
Unused land	0.7	0.7	0.7	0.6	0.7	0.7	0.6	0



In the process of optimization, each gene or LUZ is set as an integer ranging from 1 to the total number of possible land uses. The GA usually begins with 100 randomly generated plans as one generation, and those plans satisfying the defined constraints are then ordered by fitness. A second set of 100 plans is then obtained via selection, crossover, mutation, and elitism processes. These processes are used to generate subsequent generations until the degree of improvement in the average fitness of each generation is less than a certain threshold. Details of the selection, crossover, mutation, and elitism processes are as follows. (1) Selection: Two plans with a high degree of fitness are selected from randomly generated feasible plans and set as the father and mother. (2) Crossover: Genes in the two parents are exchanged via a crossover to generate children. (3) Mutation: Then, to avoid a local optimum, a process of mutation is conducted, with a mutation probability of 0.05 performed on all child plans. For each gene, there is thus a probability of 0.05 for a random change to another land-use value. These three processes are repeated until 100 plans are generated. (4) Elitism: Finally, to maintain quality, about 10 % of the plans with the highest degree of fitness in the previous generation are maintained in the next.

In the GA process, the fitness of each plan plays an important role in the selection of the father and mother. There are numerous means to compute fitness (Hajela and Lin 1992, Konak et al. 2006). In this study, the Maximin fitness function proposed by Balling (2002) is employed to measure the goodness of each plan in one generation. First, translate all objectives into the format of “min(Z),” and then let  $Ob_{ki}$  as the value of the  $k$ -th objective in the  $i$ -th plan. As for the max(Z) format objective, the objective will be transformed min(Z) format by following equation.

$$Z = -Z \tag{12}$$

Now consider two plans in one generation, the  $i$ -th plan and the  $j$ -th plan. The  $i$ -th plan will be dominate There are numerous means to compute fitness, like ranking, normalized sum objectives, weighted average of normalized objectives (Hajela and Lin 1992, Konak et al. 2006). In this study, the Maximin fitness function proposed by Balling (2002) is employed to measure the goodness of each plan in one generation. First, translate all objectives into the format of “min(Z),” and then let  $Ob_{ki}$  as the value of the  $k$ -th objective in the  $i$ -th plan. As for the max(Z) format objective, the objective will be transformed min(Z) format by following equation.

$$Z = -Z \tag{13}$$

Now consider two plans in one generation, the  $i$ -th plan and the  $j$ -th plan. The  $i$ -th plan will be dominated by the  $j$ -th plan if:

$$Ob_{1i} > Ob_{1j}, Ob_{2i} > Ob_{2j}, \dots, Ob_{ki} > Ob_{kj} \tag{14}$$

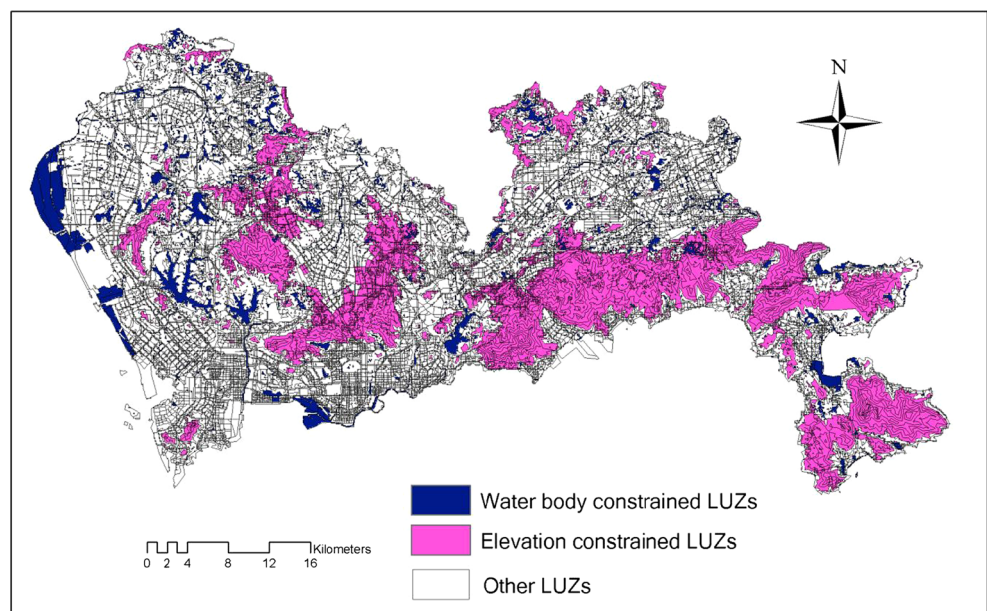
And this equation is equivalent to the following equation:

$$\min(Ob_{1i}-Ob_{1j}, Ob_{2i}-Ob_{2j}, \dots, Ob_{ki}-Ob_{kj}) > 0 \tag{15}$$

Thus, the  $i$ -th plan is a dominated plan if:

$$\max_{i \neq j} (\min(Ob_{1i}-Ob_{1j}, Ob_{2i}-Ob_{2j}, \dots, Ob_{ki}-Ob_{kj})) > 0 \tag{16}$$

**Fig. 4** Land-use zones divided by the road network and contour lines with a 75-m interval



And the fitness of the  $i$ -th plan is:

$$f_i = \left[ 1 - \max_{j \neq i} \left( \min \left( \frac{Ob_{1i} - Ob_{1j}}{Ob_{1-\max} - Ob_{1-\min}}, \dots, \frac{Ob_{ki} - Ob_{kj}}{Ob_{k-\max} - Ob_{k-\min}} \right) \right) \right]^p \quad (17)$$

In above equations, the scaling factors  $Ob_{k-\max}$  and  $Ob_{k-\min}$  are the maximum and minimum value of the  $k$ -th objective. According to Eq. 17, the fitness of Pareto-optimal plans will be between 1 and  $2^p$ , whereas the fitness of dominated plans will be between 0 and 1. As for the exponent  $p$ , if it is larger than 1, it will make the fitness of Pareto-optimal plans even higher and the fitness of dominated plans even lower. In Balling's study, he used a high value of  $p$  which was 15, and it made the GA quite aggressive in pursuing Pareto-optimal solutions (Balling et al. 1999).

In above equations, the scaling factors  $Ob_{k-\max}$  and  $Ob_{k-\min}$  are the maximum and minimum value of the  $k$ -th objective. According to Eq. 15, the fitness of Pareto-optimal plans will be between 1 and  $2^p$ , whereas the fitness of dominated plans will be between 0 and 1. As for the exponent  $p$ , if it is larger than 1, it will make the fitness of Pareto-optimal plans even higher and the fitness of dominated plans even lower. In Balling's study, he used a high value of  $p$  which was 15, and it made the GA quite aggressive in pursuing Pareto-optimal solutions (Balling et al. 1999).

## Results and discussion

### Soil erosion evaluation

Shenzhen's total soil loss was obtained using the USLE. According to the national soil erosion classification standard (SL190-2007 2008), soil erosion can be classified into six clusters based on the annual soil loss amount (tonnes per hectare). Annual soil loss of less than 5 tonnes per hectare is classified as very low, a loss ranging from 5 to 25 tonnes per hectare is classified as low, a loss ranging from 25 to 50 tonnes per hectare is classified as moderate, a loss ranging from 50 to 80 tonnes per hectare is classified as moderately high, a loss

ranging from 80 to 150 tonnes per hectare is classified as high, and a loss greater than 150 tonnes per hectare is classified as very high. Table 6 shows the percentage in Shenzhen that fell into these six clusters from 1996 to 2008. It can be seen that the degree of soil erosion was "very low" in 77.2–86.0 % of Shenzhen's total land area during this period, although some areas were classified as suffering from "high" and "very high" degrees. The area of severe soil erosion varied from year to year, in line with land-use changes and changes in the amount of precipitation from year to year. Table 6 shows the annual soil losses in 2000 and 2008 to have been much greater than those in the other years because the annual rainfall levels in these 2 years were also higher. These results indicate that the amount of precipitation determines the total amount of soil lost in a given year and that that amount can vary significantly from year to year.

The soil erosion classification map in Fig. 5 provides a visual understanding of soil erosion in Shenzhen. In line with the city's topography, it can be seen that the areas suffering the most severe soil erosion are usually those with steep slopes. It appears that variations in slope and elevation from place to place have a great effect on soil erosion.

Local policy considers an area in which the amount of soil loss is greater than 20 tonnes per hectare to be suffering from soil erosion. According to a report from the Shenzhen Municipal Water Authority, a total of 80.26 square kilometers suffered erosion in 2004 (Li et al. 2013; Mu et al. 2010). Summing areas with soil losses greater than 20 tonnes per hectare on the soil erosion map generated by the USLE model indicate that a land area equal to 82.13 square kilometers in Shenzhen is suffering from soil erosion, which suggests that the model is reasonable for assessing soil erosion in this city.

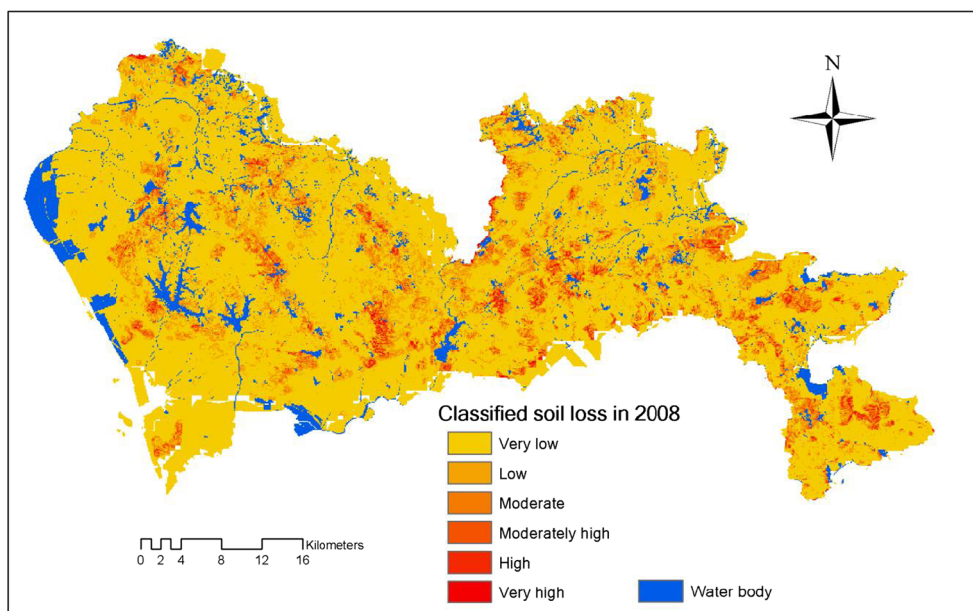
### Spatial land-use optimization

An optimal spatial land-use allocation should be capable of mitigating soil erosion according to the spatial and quantitative distribution of different land-use types in space. However, the distribution of land-use types is also determined by other objectives. Because these competing objectives are in conflict with one another, it is impossible to achieve one best solution,

**Table 6** Areas of classified soil loss from 1996 to 2008 by USLE [km<sup>2</sup>]

Year	Very low	Low	Moderate	Moderately high	High	Very high
1996	81.04	13.80	3.40	1.18	0.50	0.07
2000	77.18	15.33	4.11	1.91	1.15	0.31
2002	81.77	13.01	3.29	1.21	0.61	0.11
2004	85.99	10.88	2.30	0.59	0.22	0.02
2006	81.99	12.76	3.28	1.24	0.63	0.12
2008	78.61	14.24	3.79	1.86	1.16	0.35

**Fig. 5** Classified soil loss in Shenzhen in 2008



that is, one in which all objectives are better than or no worse than those of another. However, the GA provides a set of Pareto-optimal solutions rather than one specific solution. Figure 6 presents the Pareto-optimal solutions and Pareto line of the first and last generations. The Pareto line is the line that connects all Pareto-optimal solution points. In Fig. 6, the values of the cost of change and incompatibility act as the x and y axes, respectively.

A number of observations can be made. First, all of the solutions in the last generation are closer to coordinate point (0,0), which means that the values of both the cost of change and incompatibility are reduced by optimization. Because the GA achieves optimization by selecting plans with a greater degree of fitness to generate the next generation, the degree of fitness becomes increasingly high from generation to

generation. Through this process, the objective values of the plans in the last generation are smaller than those of the plans in the first generation, as reflected in Fig. 6.

Second, because the Pareto-optimal solutions in all of the plans in the last generation are made visual, again as shown in Fig. 6, decision-makers and planners can weigh up the importance of different objectives and then select one solution on the Pareto line. For example, if decision-makers consider incompatibility to be a much more important objective than reducing the cost of change, then they can select the Pareto-optimal solutions with the lowest incompatibility value even if those solutions have large cost-of-change values.

Third, according to the Pareto line in Fig. 6, the objective values of the cost of change and incompatibility grow smaller from the first to the last generation. Figure 7 confirms this

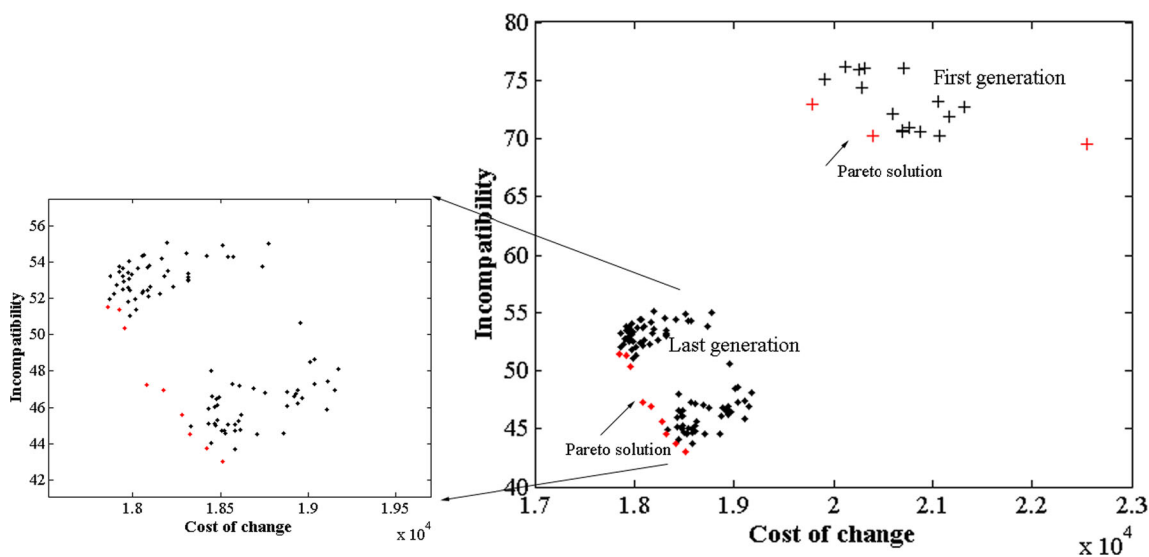


**Fig. 6** Pareto line of optimal land-use plans: the x axis is the value of the cost of change, and the y axis is the value of incompatibility

decrease in all objective values during the process of optimization, where the  $x$  axis is the iteration time of optimization, and the  $y$  axis is the average value of a particular objective for 100 plans in one generation. The objective values are dramatically reduced during the first 300 generations, which suggests that all objectives have been optimized, whereas competition among objectives occurs after the 300th generation. For example, there is a small peak in the soil-loss value around the 500th generation, whereas a valley emerges around this generation in the cost-of-change value. The competition between these two objectives is obvious, and a win–win situation is impossible. Finally, the values of all objectives tend toward convergence.

To come to a better understanding of the Pareto-optimal solutions, two group plans were selected and analyzed. In the first group, three Pareto-optimal plans that had been implemented via multi-objective optimization maintained minimum objective values for the cost of change, land-use incompatibility, and soil erosion. They are listed as Plans 1, 2, and 3 in Table 7. In the second group, three plans were implemented via single-objective optimization, each of them taking one objective from the cost of change, land-use incompatibility, and soil erosion as the single objective. These three plans appear as Plans 4, 5, and 6 in Table 7. Single-objective optimization here denotes the same process as multi-objective optimization, although only one objective is considered with other two being ignored.

In the first group, there is no best solution in terms of the three objectives, the competition among which is confirmed by Fig. 7. For example, plan 1 features the lowest value for the cost of a change to the status quo, but much higher values for incompatibility and soil loss, whereas plan 2 boasts the lowest value for incompatibility but higher cost-of-change and soil-loss values than those in plans 1 and 3.

In the second group, each plan maintained one lowest value for a single objective, with the values of the other two objectives larger in comparison. Take Plan 4 as an example. It is the optimized result achieved by considering the single objective cost of change and maintains the lowest value for this cost, 16,753.40. This value is lower than those of all plans in both the first (the Pareto plans) and second groups. However,

because Plan 4 takes minimization of the cost of change as its single objective, while ignoring the other two objectives, i.e., incompatibility and soil erosion, those two minimizing

**Table 7** Objective values of three selected plans

Land-use plan	Cost of change to status quo	Incompatibility	Soil loss [t/ha]
Plan 1	18,863.30	46.51	0.7687
Plan 2	18,974.50	42.51	0.7601
Plan 3	19,053.00	44.88	0.7595
Plan 4	16,753.40	74.40	0.8604
Plan 5	20,341.40	37.30	0.8714
Plan 6	19,458.50	73.67	0.7110

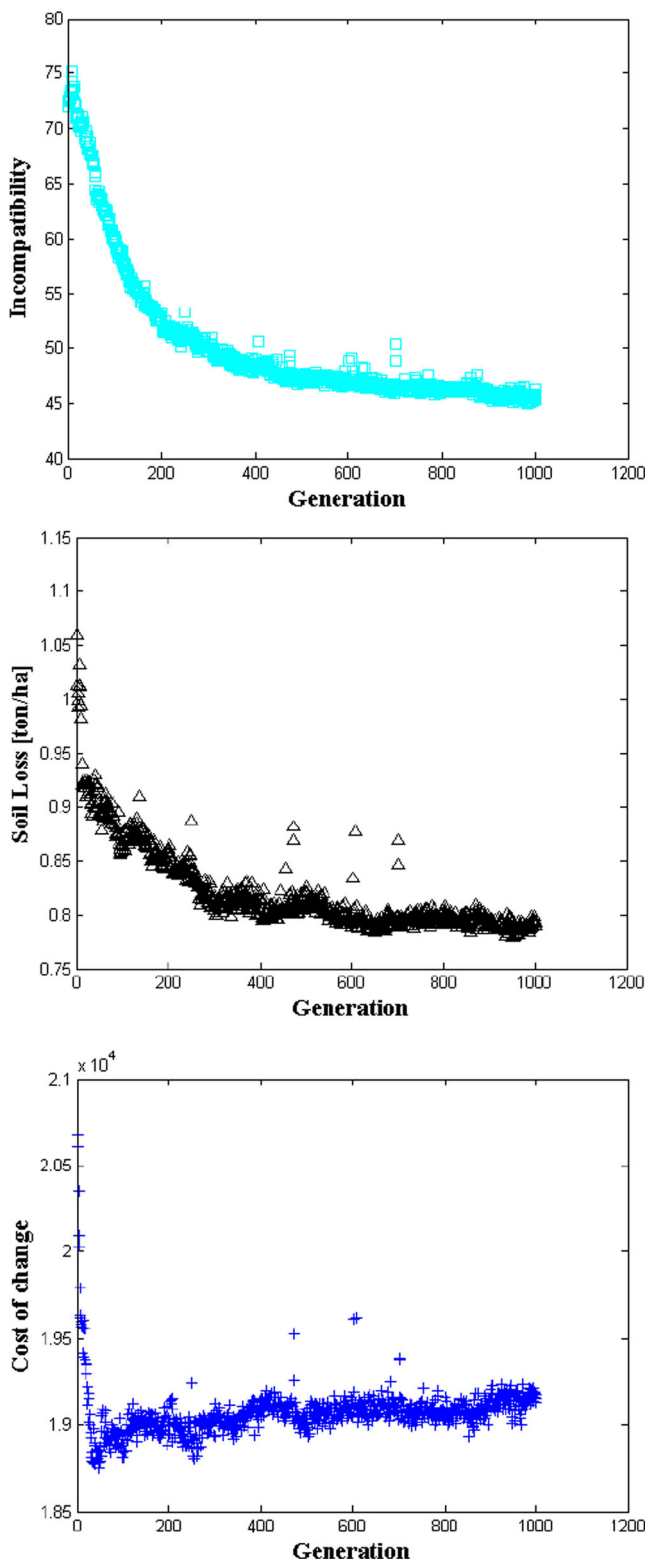


**Fig. 7** Variations in objective value from the first to final generations

**Table 8** Land-use areas of three selected plans

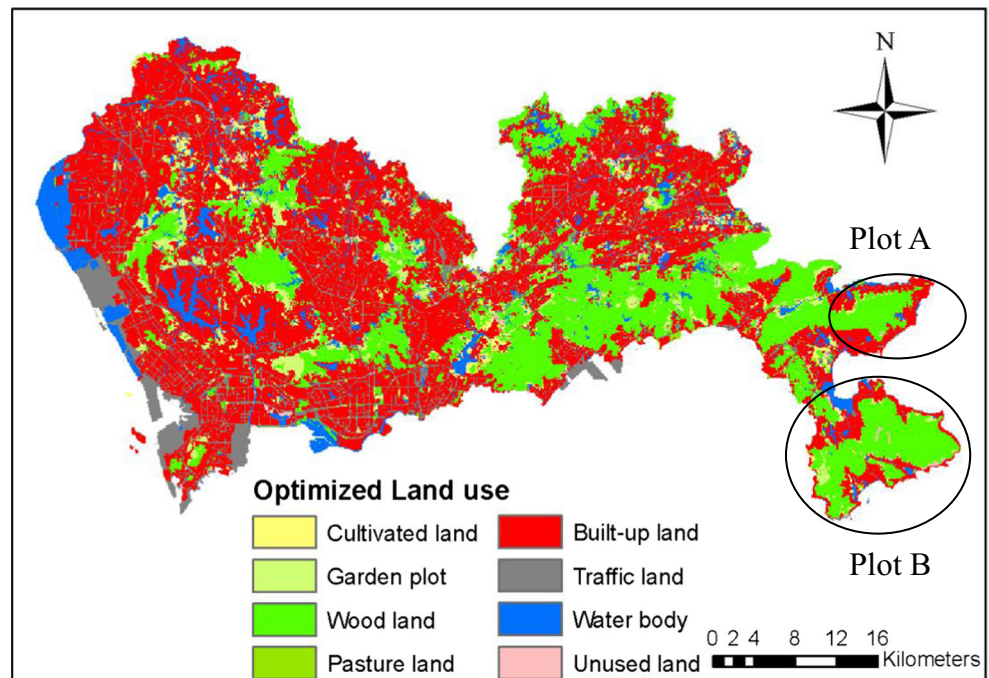
Land-use types	Plan 1 Area [km <sup>2</sup> ]	Plan 2	Plan 3	Constraints
Cultivated land	30.69	31.22	32.19	> 25.65 km <sup>2</sup>
Garden plot	99.46	97.88	96.96	
Forest	457.53	457.89	456.53	
Grassland	13.09	12.56	12.58	
Built-up land	991.87	992.13	993.15	> 990 km <sup>2</sup>
Transportation	203.18	203.32	203.50	
Water body	141.34	141.34	141.34	= 141.34 km <sup>2</sup>
Unused land	15.67	16.49	16.60	
Sum	1,952.84			

objectives are relatively large. More specifically, Plan 4 maintains an incompatibility value of 74.4, whereas the Pareto plans maintain incompatibility values ranging from 42.51 to 46.51 and a soil loss value of 0.8604 t/ha, whereas the Pareto plans undergo soil loss ranging from 0.7595 to 0.7687 t/ha. Obviously, the single-objective plans maintain a minimum objective value for a single objective, whereas the other two objectives are ignored and are thus relatively large. Comparison of the Pareto solutions with the results achieved via single-objective optimization shows that, although multi-objective optimization is unable to achieve the best solution for each single objective, it is able to make a tradeoff among all conflicting objectives and attempt to find some Pareto solutions.

The quantitative areas of all land-use types in the first-group three plans are listed in Table 8. All of the plans satisfy the constraints because the optimization process in the GA is conducted only for plans that previously satisfied the constraints. Although there are few differences among the three plans, similar land-use areas generate numerous spatial allocation scenarios, which lead to a gap in the plans' objectives.

Figure 8 shows the spatial distribution of the plan with the lowest objective value for soil loss as an example. Compared with the land-use pattern in 2008 (see Fig. 2), an increase in the amount of built-up land can be seen because the constraint on built-up land to accommodate population growth and economic development in Shenzhen is around 990 km<sup>2</sup>, and the total built-up land area in 2008 was 754.43 km<sup>2</sup>. The optimization process thus adds about 236 km<sup>2</sup> of built-up land. More specifically, the built-up land in Fig. 8 tends to increase around the administrative boundaries of Shenzhen. With regard to the spatial distribution of slope and elevation in Shenzhen, it can be seen that the additional built-up land is generally allocated to areas with a low elevation and plain slope, which should relieve the severity of soil erosion to some extent. The increases in built-up land are also clustered (see Plots A and B in Fig. 8) because of the objective to minimize land-use incompatibility in a given neighborhood. Clustered built-up land leads to minimal such incompatibility. Finally, because an increase in built-up land acts as a constraint that must be satisfied first, the objective of minimizing the cost of changes to the status quo can be considered after a land-use plan requiring such an increase has been formulated.

**Fig. 8** Spatial distribution of optimized land-use plan with lowest soil erosion value



## Summary and conclusions

The paper presents the results of the computation and analysis of soil erosion with regard to land-use changes in a rapidly urbanizing city using the USLE model with the assistance of GIS and RS techniques. The USLE model was used to calculate the annual soil loss in Shenzhen based on soil type, precipitation, vegetation cover, slope, and land-use status. In the process of evaluation, the GIS and RS techniques were used to collect and present the spatial factors and results. The results of the USLE model were validated using statistical soil loss data from 2004. The spatial results show a steep slope to have a huge effect on soil loss, whereas the total amount of soil lost each year suggests that annual precipitation exerts only a temporary effect on such loss. At the same time, because land-use change leads to a varying crop and management factor  $C$  and conservation practice factor  $P$ , and the slope is the result of natural characteristics and uncontrollable precipitation, land-use change exerts a huge impact on the total amount and spatial distribution of soil erosion in Shenzhen. The USLE model is an empirical model that allows the prediction of average annual soil loss based on the product of five erosion risk factors. Owing to difficulties in data collection, only 2004 soil loss data from Shenzhen were used to validate the model. The results suggest that the USLE model is applicable to the case study area.

In addition to soil erosion evaluation, the GA-based MOO approach was used to search for an optimal land-use plan for Shenzhen. Three objectives, one of them soil-loss minimization, and four constraints were considered. The Pareto-optimal solutions generated by the GA provided a set of alternative choices for decision-makers and land-use planners. The Pareto line makes comparison among these solutions easy. The objective values of three selected Pareto-optimal solutions were subjected to careful analysis, the results of which indicated conflict and competition among the objectives in the process of optimization. In summary, the optimization results confirm the usefulness of GA-based MOO for land-use planning optimization in Shenzhen. Such optimization allows a tradeoff among multiple objectives and constraints such as maintaining sufficient built-up land to accommodate an increasing population, reducing conflicts between neighboring land-use types, and minimizing soil loss during the process of urbanization.

Urbanization is a growing trend worldwide. Take China as an example. Its national urbanization level stood at 11 % in 1949 and at 29 % in 1996 (Wang et al. 2004). The aggravating role that urban sprawl and natural land disappearance play in soil erosion is obvious and has been confirmed in numerous studies (Van Hengstum et al. 2007; Fistikoglu and Harmancioglu 2002; Yang et al. 2003; Lufafa et al. 2003). Therefore, a comprehensive evaluation of soil erosion taking temporal and spatial land-use changes into account is

necessary, particularly for cities located in mountainous areas with high levels of rainfall. Such cities also require sound land-use plans that take soil erosion control into consideration. The GA-based MOO approach used in the study reported herein is capable of taking the spatially related and complex objective of soil erosion control into account. Most importantly, the optimal plans generated by MOO offer alternatives to decision-makers and planners who can choose from among a number of Pareto-optimal solutions. Furthermore, for the greater convenience of decision-makers, the spatial distribution of alternative plans can be represented by the GIS tool, with the specific objective values of each plan also provided. With the help of the GIS tool, the MOO approach renders land-use planning system simpler and makes it easier to formulate sound and practical land-use plans.

## References

- Abu Hammad A (2011) Watershed erosion risk assessment and management utilizing revised universal soil loss equation–geographic information systems in the Mediterranean environments. *Water Environ J* 25(2):149–162
- Aerts JC, Eisinger E, Heuvelink G, Stewart TJ (2003) Using linear integer programming for multi-site land-use allocation. *Geogr Anal* 35(2):148–169
- Balling R (2002) The maximin fitness function for multiobjective evolutionary optimization. *Optimization in Industry*, Springer 135–147
- Balling R, Taber JT, Brown MR, Day K (1999) Multiobjective urban planning using genetic algorithm. *J Urban Plan Dev* 125(2):86–99
- Balling R, Powell B, Saito M (2004) Generating future land-use and transportation plans for high-growth cities using a genetic algorithm. *Comput Aided Civ Infrastruct Eng* 19(3):213–222
- Balling R, Wilson S (2001) The maxi-min fitness function for multi-objective evolutionary computation: application to city planning. *Proceedings of the Genetic and Evolutionary Computation Conference (GECCO'2001)*
- Cai C, Ding S, Shi Z, Huang L, Zhang G (2000) Study of applying USLE and geographical information system IDRISI to predict soil erosion in small watershed. *J Soil Water Conserv* 14(2):19–24
- Cao K, Batty M, Huang B, Liu Y, Yu L, Chen J (2011) Spatial multi-objective land use optimization: extensions to the non-dominated sorting genetic algorithm-II. *Int J Geogr Inf Sci* 25(12):1949–1969
- Cao K, Huang B, Wang S, Lin H (2012) Sustainable land use optimization using boundary-based fast genetic algorithm. *Comput Environ Urban Syst* 36(3):257–269
- Chen DY, Yang DS, Xiao WG, Wu CW (2001) Application of SPOT remote sensing data to the survey of soil erosion status in Shenzhen. *Pearl River* 22(05):55–57
- Chen Z, Gong C, Wu J, Yu S (2012) The influence of socioeconomic and topographic factors on nocturnal urban heat islands: a case study in Shenzhen, China. *Int J Remote Sens* 33(12):3834–3849
- Dumas P, Printemps J, Mangeas M, Luneau G (2010) Developing erosion models for integrated coastal zone management: a case study of The New Caledonia west coast. *Mar Pollut Bull* 61(7):519–529
- Fistikoglu O, Harmancioglu NB (2002) Integration of GIS with USLE in assessment of soil erosion. *Water Resour Manag* 16(6):447–467

- Guldmann J-M (1979) Urban land use allocation and environmental pollution control: an intertemporal optimization approach. *Socio Econ Plan Sci* 13(2):71–86
- Hajela P, Lin C-Y (1992) Genetic search strategies in multicriterion optimal design. *Struct Optim* 4(2):99–107
- Holzkämper A, Seppelt R (2007) A generic tool for optimising land-use patterns and landscape structures. *Environ Model Software* 22(12):1801–1804
- Hopkins L (1977) Land-use plan design—quadratic assignment and central-facility models. *Environ Plan A* 9(6):625–642
- Kim JB, Saunders P, Finn JT (2005) Rapid assessment of soil erosion in the Rio Lempa Basin, Central America, using the universal soil loss equation and geographic information systems. *Environ Manag* 36(6):872–885
- Konak A, Coit DW, Smith AE (2006) Multi-objective optimization using genetic algorithms: a tutorial. *Reliab Eng Syst Saf* 91(9):992–1007
- Kumar S, Kushwaha S (2013) Modeling soil erosion risk based on RUSLE-3D using GIS in a Shivalik sub-watershed. *J Earth Syst Sci* 1–10
- Lal R (1995) Global soil erosion by water and carbon dynamics. *Soils Glob Chang* 131–142
- Lal R, Bruce J (1999) The potential of world cropland soils to sequester C and mitigate the greenhouse effect. *Environ Sci Pol* 2(2):177–185
- Lee S (2004) Soil erosion assessment and its verification using the universal soil loss equation and geographic information system: a case study at Boun, Korea. *Environ Geol* 45(4):457–465
- Li JJ, Wang YL, Li DQ, Zhuo ML, Wu JS (2013) Characterization and evaluation of agricultural soil erosion in Shenzhen City using environmental radionuclides. *Res Environ Sci* 26(7):780–786
- Li T, Li W, Qian Z (2010) Variations in ecosystem service value in response to land use changes in Shenzhen. *Ecol Econ* 69(7):1427–1435
- Li Y, Liu C, Yuan X (2009) Spatiotemporal features of soil and water loss in three gorges reservoir area of Chongqing. *J Geogr Sci* 19(1):81–94
- Ligmann-Zielinska A, Church R, Jankowski P (2005) Sustainable urban land use allocation with spatial optimization. Conference Proceedings. The 8th International Conference on Geocomputation
- Ligmann-Zielinska A, Church RL, Jankowski P (2008) Spatial optimization as a generative technique for sustainable multiobjective land-use allocation. *Int J Geogr Inf Sci* 22(6):601–622
- Los M (1978) Simultaneous optimization of land-use and transportation—synthesis of quadratic assignment problem and optimal network problem. *Reg Sci Urban Econ* 8(1):21–42
- Lufafa A, Tenywa M, Isabirye M, Majaliwa M, Woome P (2003) Prediction of soil erosion in a Lake Victoria basin catchment using a GIS-based universal soil loss model. *Agric Syst* 76(3):883–894
- Ma CF, Ma JW, Buhe-Aosaier (2001) Quantitative assessment of vegetation coverage factor in USLE model using remote sensing data. *Bull Soil Water Conserv* 21(4):6–9
- McCool D, Brown L, Foster G, Mutchler C, Meyer L (1987) Revised slope steepness factor for the Universal soil loss equation. *American Society of Agricultural Engineers, Transactions TAAEJ* 30(5)
- Meusburger K, Konz N, Schaub M, Alewell C (2010) Soil erosion modelled with USLE and PESERA using QuickBird derived vegetation parameters in an alpine catchment. *Int J Appl Earth Obs Geoinf* 12(3):208–215
- Meyer WB, Turner BL II (1994) *Changes in land use and land cover: a global perspective*. Cambridge University Press, Cambridge
- Mu TL, Xie J, Wu JS, Wang XR, Zheng MK (2010) Effects of land use on soil erosion in Shenzhen, China. *Res Soil Water Conserv* 3:012
- Nachtergaele F, Van Velthuizen H, Verelst L (2008) *Harmonized world soil database*. Food and Agriculture Organization of the United Nations
- Ning S-K, Chang N-B, Jeng K-Y, Tseng Y-H (2006) Soil erosion and non-point source pollution impacts assessment with the aid of multi-temporal remote sensing images. *J Environ Manag* 79(1):88–101
- Oh J, Jung S (2005) Potential soil prediction for land resource management in the Nakdong River basin. *J Korea Soc Rural Plan* 11(2):9–19
- Ozcan AU, Erpul G, Basaran M, Erdogan HE (2008) Use of USLE/GIS technology integrated with geostatistics to assess soil erosion risk in different land uses of Indagi Mountain Pass—Cankırı, Turkey. *Environ Geol* 53(8):1731–1741
- Ozsoy G, Aksoy E, Dirim MS, Tumsavav Z (2012) Determination of soil erosion risk in the Mustafakemalpaşa River Basin, Turkey, using the revised universal soil loss equation, geographic information system, and remote sensing. *Environ Manag* 50(4):679–694
- Park S, Oh C, Jeon S, Jung H, Choi C (2011) Soil erosion risk in Korean watersheds, assessed using the revised universal soil loss equation. *J Hydrol* 399(3–4):263–273
- Pimentel D (1993) *World soil erosion and conservation*. Cambridge University Press, Cambridge
- Pimentel D, Harvey C, Resosudarmo P, Sinclair K, Kurz D, McNair M, Crist S, Shpritz L, Fitton L, Saffouri R (1995) *Environmental and economic costs of soil erosion and conservation benefits*. Science—New York Then Washington 1117–1117
- Sharpley A N, Williams J R (1990) EPIC-erosion/productivity impact calculator: 1. Model documentation. Technical Bulletin—United States Department of Agriculture (1768 Pt 1)
- SL190-2007 (2008) *Standards for classification and gradation of soil erosion*. M. o. w. r. o. t. p. s. R. o. China
- Shenzhen Statistics Bureau (1997) *Shenzhen statistic yearbook*. China Statistics Press, Beijing
- Shenzhen Statistics Bureau (2001) *Shenzhen statistic yearbook*. China Statistics Press, Beijing
- Shenzhen Statistics Bureau (2003) *Shenzhen statistic yearbook*. China Statistics Press, Beijing
- Shenzhen Statistics Bureau (2005) *Shenzhen statistic yearbook*. China Statistics Press, Beijing
- Shenzhen Statistics Bureau (2007) *Shenzhen statistic yearbook*. China Statistics Press, Beijing
- Shenzhen Statistics Bureau (2009) *Shenzhen statistic yearbook*. China Statistics Press, Beijing
- Stewart TJ, Janssen R, van Herwijnen M (2004) A genetic algorithm approach to multiobjective land use planning. *Comput Oper Res* 31(14):2293–2313
- Tsyganok VV, Kadenko SV, Andriichuk OV (2012) Significance of expert competence consideration in group decision making using AHP. *Int J Prod Res* 50(17):4785–4792
- Van Hengstum P, Reinhardt E, Boyce J, Clark C (2007) Changing sedimentation patterns due to historical land-use change in Frenchman’s Bay, Pickering, Canada: evidence from high-resolution textural analysis. *J Paleolimnol* 37(4):603–618
- Wang Z, Bai Z, Yu H, Zhang J, Zhu T (2004) Regulatory standards related to building energy conservation and indoor-air-quality during rapid urbanization in China. *Energy Build* 36(12):1299–1308
- Wischmeier WH (1976) Use and misuse of universal soil loss equation. *J Soil Water Conserv* 31(1):5–9
- Wischmeier W H, Smith D D (1961) A universal equation for predicting rainfall erosion losses—an aid to conservation farming in humid regions. US Dept. of Agric., Agr. Res. Serv. ARS Special Report 22–66
- Wischmeier W H, Smith D D (1978) *Predicting rainfall erosion losses—a guide to conservation planning*.
- Wu L, Long T-Y, Cooper WJ (2012) Temporal and spatial simulation of adsorbed nitrogen and phosphorus nonpoint source pollution load in

- Xiaojiang watershed of three gorges reservoir area, China. *Environ Eng Sci* 29(4):238–247
- Xu Y, Li T (1999) Dynamic evaluation of soil erosion in Shenzhen based on land-use structural variation. *J Yangtze River Sci Res Inst* 26(7):6–12
- Yang D, Kanae S, Oki T, Koike T, Musiak K (2003) Global potential soil erosion with reference to land use and climate changes. *Hydrol Process* 17(14):2913–2928
- Zhang H, Zeng Y, Bian L (2010) Simulating multi-objective spatial optimization allocation of land use based on the integration of multi-agent system and genetic algorithm. *Int J Environ Res* 4(4): 765–776
- Zhao YX, Zhang WS, Wang Y, Wang TT (2007) Soil erosion intensity prediction based on 3S technology and the USLE: a case from Qianqeng Reservoir Basin in Shenzhen [J]. *J Subtrop Resour Environ* 3:006
- Zhou W, Xie S, Zhu L, Tian Y, Yi J (2008) Evaluation of soil erosion risk in Karst regions of Chongqing, China. *Opt Eng Appl* 70831E-70831E-70810